Salman AMIRKHAN, Atila SKANDARNEZHAD, Amangaldi KOOCHAKI, Ramin MOKHTARI

Department of Electrical Engineering, Aliabad Katoul Branch, Islamic Azad University, Aliabad Katoul, Iran

doi:10.15199/48.2015.10.28

A New Input Clamped Bi-directional Boost Converter for Electric Vehicle Charging with Unity Power Factor

Abstract. *This paper presents a new synchronous boost converter without input diode bridge. Also its source voltage is clamped using a capacitor. This converter employed as an electric vehicle (EV) charger. Its control circuit designed so that the converter input current is sinusoidal and in-phase with the main voltage, then its power factor (PF) reaches unity. It is able to bi-directional power flow capability. A bias capacitor connected in series with the ac source provides a dc voltage clamp at the input, thus input voltage remains always positive. This converter may be controlled to draw sinusoidal average current at the ac side that is either in-phase or any phase difference from the ac source. Hence, it can provide either unity power factor rectification or inversion. Mosfet devices with anti-parallel diodes are used as switches. The efficiency achieved was over 90% and the THD of the input current is under 3%. High frequency noise filter where is placed in the input side guarantees the electro-magnetic compatibility. This topology is superior to conventional rectifier followed by a dc/dc boost converter because of diode bridge elimination and removal of crossover distortions that are inevitable in conventional Active Power Factor Correction (APFC) circuits. Finally, the proposed converter is simulated using Psim software under the hysteresis control method. Very good agreement between the theatrical and simulation results are obtained.*

Streszczenie. *W artykulwe opisano przekształtnik typu boost bez wejściowego mostka diodowego. Przekształtnik zastosowano jako układ ładujący w pojazdach elektrycznych. Układ zaprojektowano w ten sposób że sinusoidalny prąd wejściowy jest w fazie z napięciem a więc spółczynnik mocy jest równy jedności. Kondensator na wejściu separuje składową stałą napięcia ładującego.* ***Nowy układ przekształtnika typu boost do ładowania pojazdów elektrycznych ze współczynnikiem mocy równym jeden***

Keywords: Power Factor Correction, Boost Converter, Hysteresis Converter, Electrical Vehicle.
Słowa kluczowe: przekształtnik boost, ładowanie pojazdów elektrycznycvh, korekcja współczynnika mocy.

Introduction

Power converters, controlled or uncontrolled type are the major pollutant of ac power distribution network. The increased number of industrial as well as commercial and residential power consumers with non linear input characteristics increases this problem [1], [2]. Not only the low power factor and harmonic line currents generated by conventional rectifiers but also all kinds of choppers and frequency converters contribute to this problem. New switched mode power consumers operating at mains voltage, such as electronic ballasts and fluorescent dimmers, have further increased the pollution. The harmful effects of harmonics in power systems are well known. A search for better power factor correction (PFC) circuits became a challenge for many researchers and engineers for the past two decades [3], [4].

Various topologies were found suitable for PFC circuits and some which highly depend on the feedback control to achieve low total harmonic distortion (THD) such as Boost and Flyback converters operate in continuous conduction mode (CCM). Other circuits seem to poses inherent high power factor properties like Boost and Flyback converters while operate in discontinuous conduction mode (DCM). Conventional small signal models and control theorems are difficult or impossible to apply because control parameters such as duty ratio are controlled to vary in a wide range [5].

This paper presents a new topology that is applicable for PFC circuits, which does not fit in the general description of traditional PFC schemes. A rectification diode bridge is not used to interface with the ac source that allows for power flow in both directions. It uses only two MOSFET switches with their body diodes, thus the same circuit may be operated either as a high quality rectifier or as an inverter. A previous attempt to replace the diode rectifier with a boost capacitor was based on Cuk topology implemented with bi-directional current switches. The topology proposed in this paper is based on the boost topology and is controlled using hysteresis PFC technique. This strategy implies the following advantages over the previous ones.

- Reduced order of the system (three state variables instead of four in the previous topology).
- Better stability
- Decreased component count
- Better switch utilization and reduced current stress
- Improved efficiency and power factor

The advantages and disadvantages of various control approaches have been evaluated for this topology, including hysteresis, cycle-by-cycle and averaged control. The theoretical results are validated by PSim simulations.

Proposed converter scheme

The power stage of the proposed converter is depicted in Fig.1. The ac power source is coupled to a switch via an inductor and a capacitor. The load can be either passive or active. As it can be seen, the four-diode bridge rectifier that commonly couples the ac source and the switching converter does not exist in this topology. This results in a possibility to reverse the direction of the inductor current. The output voltage is positive, therefore, the input voltage must be positive as well. A second reason requiring an always positive input voltage is the use of switches with unidirectional voltage blocking capability. It is the role of bias capacitor C_i to clamp V_i to an always positive value.

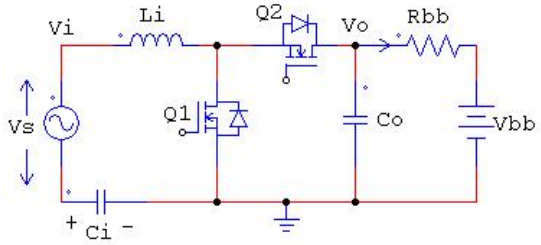

Fig.1. Usual buck converter circuit

Here Q1 and Q2 have opposite situation, when one of them is on the other one is off and vice versa. Resistor Rbb adjusts the charging current of EV batteries bank (V_{bb}).

Since the circuit is to shape the input current to a closely sinusoidal form, these switches must be able to conduct in both directions. This converter can be controlled in the appropriate manner to produce the desired input current, both capacitors C_i and C_o must be charged up to steady state values. Once the capacitors are charged to the steady state values of voltage, the following switching sequence is applied: the Q_1 and Q_2 may be driven by complimentary

signals, however, only one transistor will conduct during each line cycle, while the inductor current is alternately diverted from one switch to the anti-parallel diode of the second switch and vice versa. This is best seen in Fig. 2 where the conduction modes are presented.

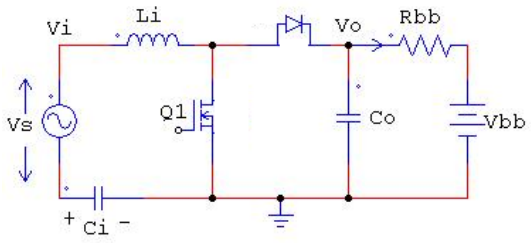

Mode1: positive half cycle

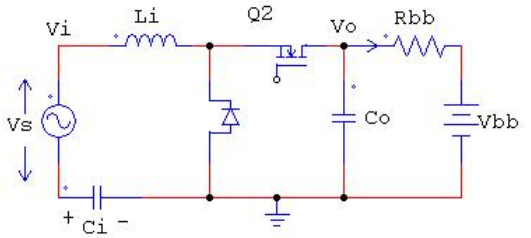

Mode2: negative half cycle

Fig.2. Two modes of the converter operation

Since the inductor current that is the input current, must follow the line voltage shape, the current is positive during the positive half cycle of the line and is negative during the negative half cycle. During the positive half period of the line voltage, the converter operates in mode 1. In this mode, power is transferred from the line voltage source and from the bias capacitor C_i to the dc output while the average input current follows V_s. During the negative half cycle the converter operates in mode 2 and drawing power from the output capacitor C_o. The average input current again follows V_s. Thus, the power drawn from V_s and V_o charges the C_i. This indicates that the input current can be controlled by alternately switching between mode 1 and mode 2 to produce the desired current shape. Specific conditions that guarantee controllability of the input current and resulting constrains which implied on the power stage are derived in the next section.

Theoretical equations of the proposed converter

The major goal of the controller is to create a resistive behaviour at the point at which the converter interfaces the line. This resistance is denoted as the emulated resistance R_{em} [6]. Here, the converter is controlled in such a way that the inductor average current follows the hysteresis band between the reference signals of I_a and I_b as seen in Fig.3.

Also Fig.3 shows the switches situation on the boundary of hysteresis band. Equation (1) represents the emulated resistance value of the converter seen from source side.

(1)
$$V_s(t) = V_m \sin(\omega t)\ ,\ I_s(t) = \frac{I_a(t) + I_b(t)}{2} \Rightarrow R_{em} = \frac{V_s(t)}{I_s(t)} = \frac{2V_m}{I_a + I_b}$$

Input voltage (Vi) instantaneous value may be derived using the following equation.

(2)
$$V_i(t) = V_{C_i}(t) + V_s(t) = V_{C_i}(0) - \frac{1}{C_i}\int_0^t I_s(t)dt + V_s(t) = V_{C_i}(0) + \frac{I_a + I_b}{2\omega C_i}(\cos(\omega t) - 1) + V_m \sin(\omega t)$$

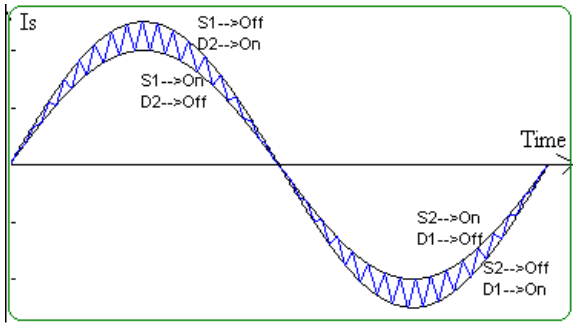

Fig.3. Switches situation on the boundary of hysteresis band

Equations (3)-(6) present the input current stable condition in four possible regions.

(3) Case I

$$\{S_1\ On, 0 < \omega t < \frac{\pi}{2}\} \| \{S_2\ Off, \frac{3\pi}{2} < \omega t < 2\pi\} \Rightarrow$$

$$\frac{dI_s(t)}{dt} \geq \frac{2dI_{avg}(t)}{dt} \Rightarrow \left(\frac{V_{C_i}(0)}{V} - \frac{1}{R_{em}\omega C_i}\right) \geq \sqrt{1 + \left(\frac{2\omega L_i}{R_{em}} - \frac{1}{R_{em}\omega C_i}\right)^2}$$

(4) Case II

$$\{S_1\ Off, 0 < \omega t < \frac{\pi}{2}\} \| \{S_2\ On, \frac{3\pi}{2} < \omega t < 2\pi\} \Rightarrow$$

$$\frac{dI_s(t)}{dt} \leq -\frac{2dI_{avg}(t)}{dt} \Rightarrow \left(\frac{V_{out} - V_{C_i}(0)}{V_m} + \frac{1}{R_{em}\omega C_i}\right) \geq \sqrt{1 + \left(\frac{2\omega L_i}{R_{em}} + \frac{1}{R_{em}\omega C_i}\right)^2}$$

(5) Case III

$$\{S_1\ On, \frac{\pi}{2} < \omega t < \pi\} \| \{S_2\ Off, \pi < \omega t < \frac{3\pi}{2}\} \Rightarrow$$

$$\frac{dI_s(t)}{dt} \geq -\frac{2dI_{avg}(t)}{dt} \Rightarrow \left(\frac{V_{C_i}(0)}{V} - \frac{1}{R_{em}\omega C_i}\right) \geq \sqrt{1 + \left(\frac{2\omega L_i}{R_{em}} + \frac{1}{R_{em}\omega C_i}\right)^2}$$

(6) Case IV

$$\{S_1\ Off, \frac{\pi}{2} < \omega t < \pi\} \| \{S_2\ On, \pi < \omega t < \frac{3\pi}{2}\} \Rightarrow$$

$$\frac{dI_s(t)}{dt} \leq \frac{2dI_{avg}(t)}{dt} \Rightarrow \left(\frac{V_{out} - V_{C_i}(0)}{V_m} + \frac{1}{R_{em}\omega C_i}\right) \geq \sqrt{1 + \left(-\frac{2\omega L_i}{R_{em}} + \frac{1}{R_{em}\omega C_i}\right)^2}$$

By combination of Equations (3) and (5) one can easily deduce the maximum value of the input capacitor voltage that is expressed in the following equation.

(7)
$$\frac{V_{C_i}(0)}{V_m} \geq \left(\sqrt{1 + \left(\frac{2\omega L_i}{R_{em}} + \frac{1}{R_{em}\omega C_i}\right)^2} + \frac{1}{R_{em}\omega C_i}\right)$$

Also by combination of Equations (4) and (6) one can easily deduce the minimum value of the input capacitor voltage where is expressed in equation (8).

(8)
$$\frac{V_{out} - V_{C_i}(0)}{V_m} \geq \left(\sqrt{1 + \left(\frac{2\omega L_i}{R_{em}} + \frac{1}{R_{em}\omega C_i}\right)^2} - \frac{1}{R_{em}\omega C_i}\right)$$

Overall control circuitry of the proposed EV charger

During the last years the interest in electric vehicles (EV) grew strongly due to ecological aspects. However, the long charging times, which usually exceed 30 minutes for a full charge, as well as the range limitation of EV's due to the available battery technology are still challenging problems. The following figure shows a typical EV general system [7].

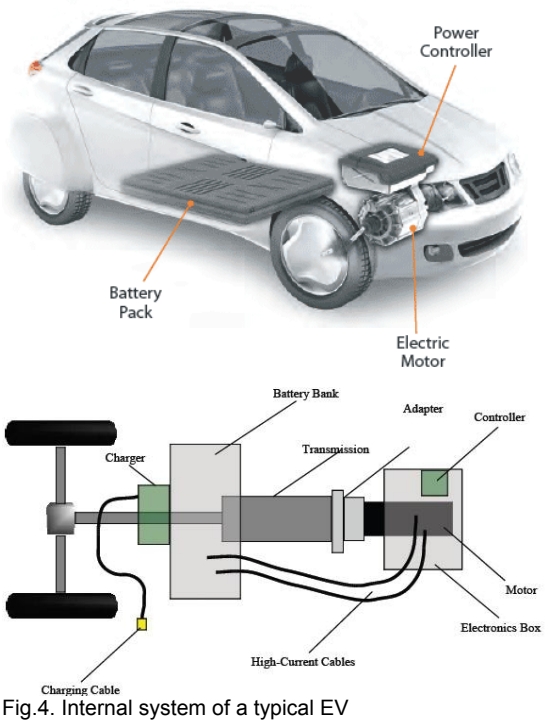

Fig.4. Internal system of a typical EV

Also the proposed converter circuit is depicted in Fig.5.

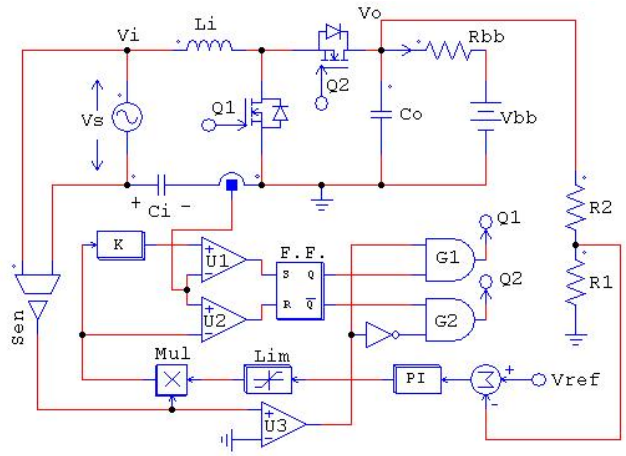

Fig.5. the closed loop converter overall circuitry

Fig.5 shows this type of control in which two sinusoidal current references are generated, one for the peak and the other for the valley of the inductor current. According to this control technique, the switch turns on when the inductor current goes below the lower reference and turns off when the inductor current goes above the upper reference giving rise to a variable frequency control. Also with this control technique the converter works in continuous conduction mode (CCM). This technique has two main advantages: I. No need of compensation ramp, and, II. Low distorted input current waveforms.

In order to avoid too high switching frequency, the switch can be kept open near the zero crossing of the line voltage so it introduces dead times in the line current [8].

A control IC which implements this control technique is the CS3810 (Cherry Semiconductor) [9]. As seen in Fig. 5, the error between output voltage (V_o) and reference (V_{ref}) has been applied to a PI compensator, and its output modulates the amplitude of reference current witch is compared with source current by U_1 and U_2. Comparator (U_3) enables (/disables) the switches gating signal in the positive (/negative) half cycles.

The size of the energy storage elements in switch mode power supplies (SMPS) decrease approximately linearly with the increase of switching frequency [10]. Therefore, high density power supplies generally demand high switching frequency and fast semiconductor devices. However, the increased switching frequency together with the increased current and voltage slew rates such as dv/dt and di/dt has bad effects on electromagnetic compatibility (EMC) performance of the power supplies [11].

This paper also uses an electro-magnetic compatibility (EMC) filter to decrease radio frequency contents of the proposed converter. A procedure to design EMC filters introduced in [11]-[13]. Conducted EMI noises, especially the common mode current flowing into the system ground via stray capacitors have been studied. The following circuit presents a typical EMC filter employed in this paper.

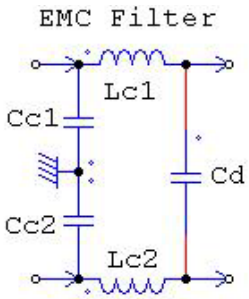

Fig.6. A typical circuit for EMC filtering

C_C and L_C are used to attenuate the common mode noise and C_d is used to differential mode respectively. This filter stays between the converter and input source. L_{C1} and L_{C2} usually are wounded on the same core; also stray inductance of them can act as an attenuator for the differential mode noise.

Simulation results

This section involves the simulation results that are done using PSim software. The task of the feedback circuit is to shape the loop gain such that its crossover frequency stays in the desired place with enough phase and gain margins for a good dynamic response, line and load regulation, and stability. First consider the converter shown in Fig.5 with values stated in Table.1.

Table1. The converter components value

Converter components		Controller components	
Part	Value	Part	Value
V_S	110V-60Hz	R_1	10KΩ
L_i	3mH	R_2	990KΩ
r_{Li}	0.1Ω	K	0.8
C_i	10mF	PI Gain	2
r_{Ci} , r_{Co}	0.05Ω	PI Time (τ)	20ms
C_o	4.7mF	Limiter	[-12:12]V
R_{bb}	10Ω	V_{ref}	4.5V
$r_{Q1,2}$	0.1Ω	$C_{C1,2}$	4.7nF
$V_{O\text{-}ref}$	450V	C_d	33nF
		$L_{C1,2}$	100uH

Converter circuit simulation with Table1 components value is done under the hysteresis control technique.

Fig.7 shows the converter input current along with its upper and lower references.

Charger output voltage is depicted in Fig.8.

Source current along with source voltage at the start-up moment is depicted in the following figure where both of them are in-phase with each other, then this reveals unity power factor.

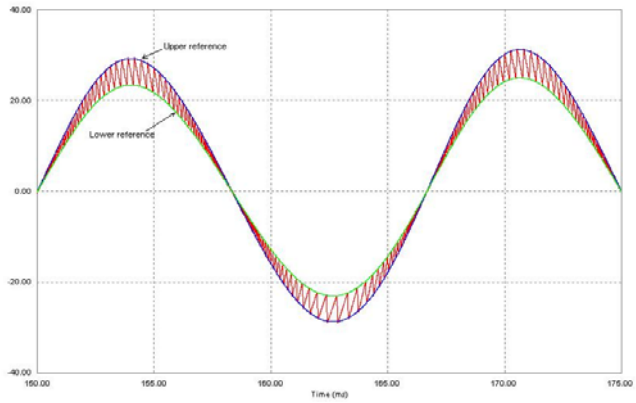

Fig.7. Converter input current

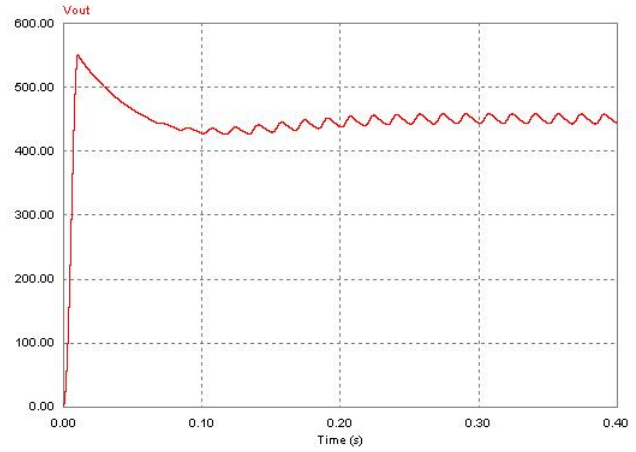

Fig.8. Converter output voltage

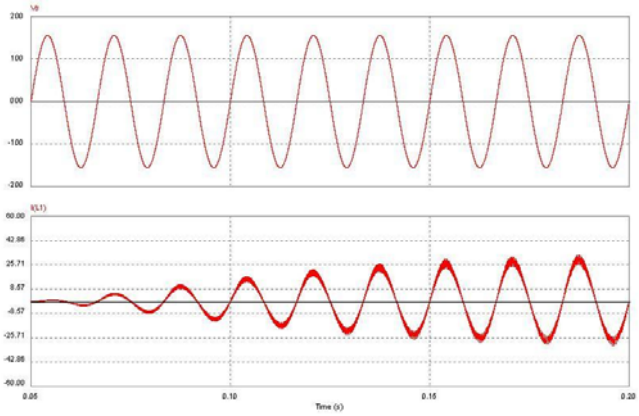

Fig.9. Source current and voltage at the start-up moment

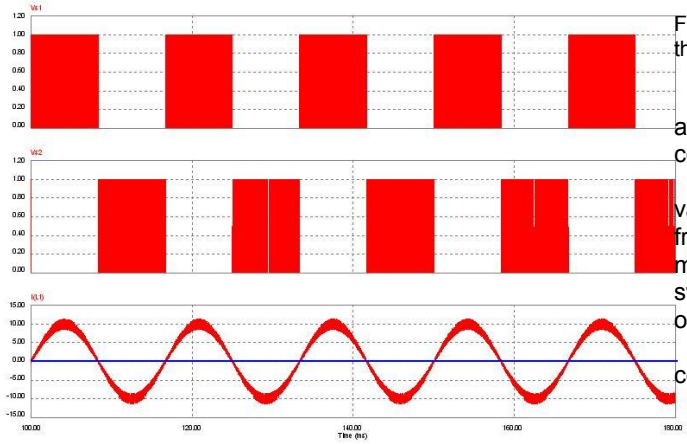

Fig.10. Driving Signals of Q_1 and Q_2

Switch's Q_1 and Q_2 work in the complementary manner. Q_1 acts in the positive half cycles and Q_2 acts in the negative half cycle of the source current. Fig.10 displays driving signals of Q_1 and Q_2 which are denoted by V_{S1} and V_{S2} respectively. As seen in figure 10, there is a little dead time between the switching signals of Q_1 and Q_2 which prevents the short circuit of the converter output capacitor.

To analyse the converter dynamic, reference voltage of output voltage is shifted deliberately from 450V to 500V. Fig. 11 shows the converter output voltage and its input current at the moment when reference voltage steps up.

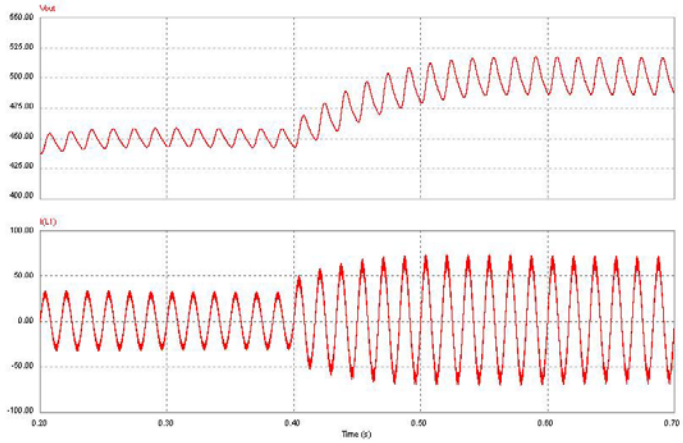

Fig.11. Converter output voltage and input current when the reference voltage changes.

In addition to power factor, total harmonic distortion (THD) is an important aspect of the switching converters. Fig. 12 exhibits the converter input current low frequency content, which its THD yielded about 3.7%.

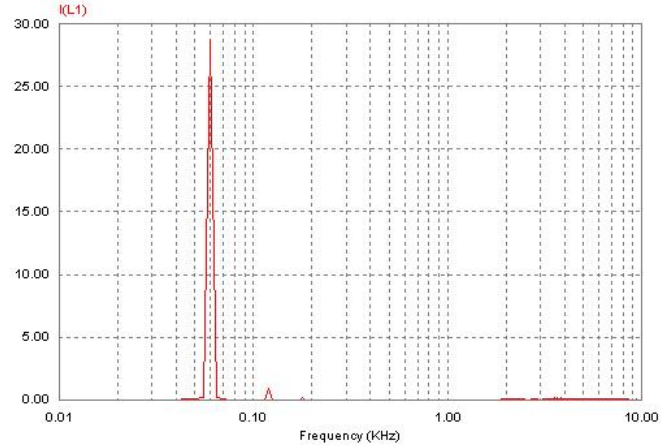

Fig.12. Frequency content of the converter input current to compute the THD factor.

EMC filter values are stated in the right column of table1 and Figure 13 shows conduction radio frequency (RF) noise contents of the converter input current with/without filtering.

Due to hysteresis method nature, switching frequency varies depending on the hysteresis band width. Maximum frequency occurs at 0^o and 180^o phases, respectively, minimum value occurs at 90^o and 270^o degree. The variable switching frequency helps to distribute the RF noise power on the frequency span and then to decrease its peak value.

Fig. 14 shows switching frequency value along with converter input current. Its peak value is about 135 kHz.

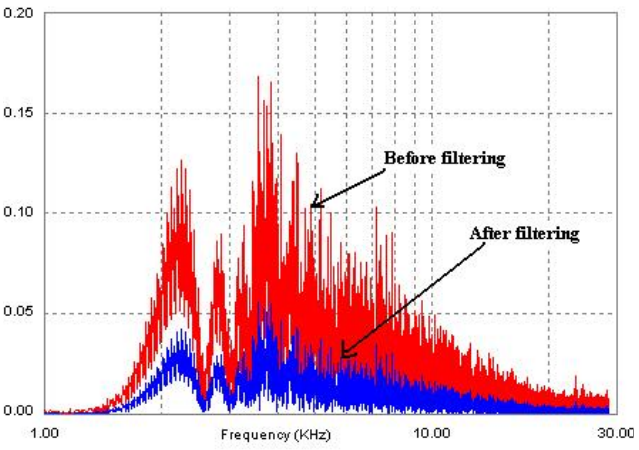

Fig.13. Radio frequency contents of input current with and without EMC filter.

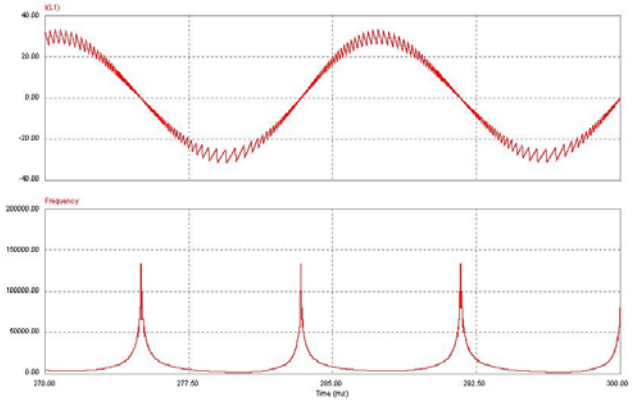

Fig.14. Switching frequency along with converter input current.

Also, Fig. 15 display the converter transistors duty cycle along with its input current.

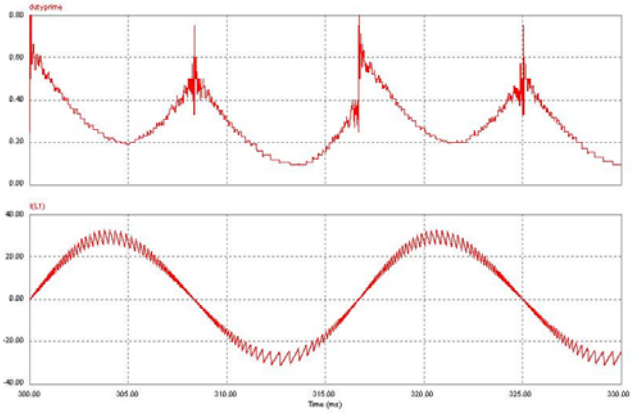

Fig.14. Switches duty cycle along with converter input current.

Minimum and maximum values of switches duty cycle help the designer to select the power and current rates of converter transistors properly. Also, these values determine the stable region for the converter feedback loop [14], [15].

Conclusion

This paper proposes a new bidirectional charger for electrical vehicle batteries with unity power factor. It uses a bias capacitor in series with the main ac source to clamp the converter input voltage to always positive values, then need for a bridge diode rectifier is eliminated. The advantages of the proposed circuit are it's the high power factor, low current THD achieved at the ac side, power stage simplicity and lower manufacturing cost. The disadvantages include: need for a large bias capacitor and large reactive components in the output filter.

Theoretical equation presented here to help designer to select the converter components value correctly. The operation mode will be selected by the hysteresis control technique precisely. Finally, this converter was validated at a medium power level by PSim simulations.

Acknowledgment

This study is extracted from research project supported by Islamic Azad University of Aliabad Katoul branch.

REFERENCES

[1] Galecki A., Kaszewski A., Grzesiak L.M., Ufnalski B., Control system of the grid-connected converter based on a state current regulator with oscillatory terms, *Przegląd Elektrotechniczny*, 01(2014), 65-69.

[2] Chen J., Chen J., Gong Ch., Meng X., Analysis and design of a novel three-level dual-boost reversible PWM rectifier, *IEEE 8th Conference on ICIEA*, 2013, 1071-1076.

[3] Gajowik T., Rafal K., Bobrowska M., Bi-directional DC-DC converter in three-phase dual active bridge topology, *Przegląd Elektrotechniczny*, 05(2014), 14-20.

[4] Yu F., Yan X., Yuwen H., A fast algorithm for SVPWM in three phase power factor correction application, *Proceedings of 35th IEEE Power Electronics Specialists Conference*, 2004.

[5] Christen D., Tschannen S., Biela J., Highly efficient and compact DC-DC converter for ultra-fast charging of electric vehicles, *IEEE 15th International Power Electronics and Motion Control Conference*, Novi Sad, Serbia, 2012, 531-538.

[6] Tollik D., Pietkiewicz A., Comparative analysis of 1-phase active power factor correction topologies, *International Telecommunication Energy Conf. Proc*., Oct. 1992, 517-523.

[7] Simonik P., Havel A., Hromjak M., Chlebis P., Active charging stations for electric vehicles charging, *Progress In Electromagnetics Research Sym. Proc.,* Malaysia, 2012, 995-998.

[8] Gautam D., Musavi F., Edington M., Eberle W., A zero voltage switching full-bridge DC-DC converter with capacitive output filter for a plug-in-hybrid electric vehicle battery charger, *IEEE Conf. of APEC,* Feb. 2012, 1381-1386.

[9] Shepherd W., Zhang L., Power Converter Circuits, *Marcel Dekker Publications*, New York, 2004.

[10] Zdanowski M., Rąbkowski J., Barlik R., High frequency DC/DC converter with Silicon Carbide devices – simulation & analysis, *Przegląd Elektrotechniczny*, 02(2014), 201-205.

[11] Guo T., Chen D.Y., Lee F.C., Separation of the common mode and differential mode conducted EMI noise, *IEEE Trans. on P.E.,* Vol.11, No.3, 1996, 480-488.

[12] Shih F.Y., Chen D.Y., Wu Y.P., Chen Y.T., A procedure for designing EMI filters for AC line applications, *IEEE Trans. on P.E.,* Vol.11, No.1,1996, 170-181.

[13] Ye S., Eberle W., Liu Y.F., A novel EMI filter design method for switching power supplies, *IEEE Trans. on P.E.,* Vol.19, No.6, 2004, 1668-1677.

[14] Basso P., Switch mode power supplies, *McGraw-Hill,* 2008.

[15] Jardini J.A., and et al., Power flow control in the converters interconnecting AC-DC meshed systems, *Przegląd Elektrotechniczny*, 01(2015), 46-49.

Authors

S. Amirkhan, A. Skandarnezhad, A. Kochaki, R. Mokhtari are all the: Assistant Professors of Electrical engineering, Department of Electrical Engineering, Aliabad Katoul Branch, Islamic Azad University, Aliabad Katoul, Iran.

*The correspondent E-mail is: amirkhan@aliabadiau.ac.ir